Anti-bacterial dynamic hydrogels prepared from O-carboxymethyl chitosan by dual imine bond crosslinking for biomedical applications

Rui Yu, Louis Cornette de Saint-Cyr, Laurence Soussan, Mihail Barboiu, S.M. Li

Anti-bacterial dynamic hydrogels prepared from O-carboxymethyl chitosan by dual imine bond crosslinking for biomedical applications

Rui Yu, Louis Cornette de Saint-Cyr, Laurence Soussan, Mihail Barboiu, Suming Li

Anti-bacterial dynamic hydrogels prepared from *O*-carboxymethyl chitosan by dual imine bond crosslinking for biomedical applications

Rui Yu, Louis Cornette de Saint-Cyr, Laurence Soussan, Mihail Barboiu *, Suming Li *

Institut Européen des Membranes, IEM UMR 5635, Univ Montpellier, CNRS, ENSCM, Montpellier, France

ARTICLE INFO

Article history:
Received 27 August 2020
Received in revised form 27 October 2020
Accepted 10 November 2020
Available online xxxx

Keywords:
O-carboxymethyl chitosan
Jeffamine
Imine bonding
pH-sensitive
Self-healing
Antibacterial property

ABSTRACT

Imine dynamic hydrogels are synthesized via dual-imine bond crosslinking from *O*-carboxymethyl chitosan (CMCS) and a water soluble dynamer using a 'green' approach. Three dynamers are prepared through reaction of benzene-1,3,5-tricarbaldehyde and di-amino Jeffamine with molar mass of 500, 800 and 1900, respectively. Hydrogels, namely H500, H800 and H1900 are then obtained by mixing CMCS and dynamer aqueous solutions. FT-IR confirms the formation of hydrogels via imine bonding. H1900 presents larger pore size and higher storage modulus as compared to H500 and H800 due to the higher molar mass of Jeffamine linker. The hydrogels exhibit pH sensitive swelling behavior due to electrostatic attraction or repulsion in the pH range from 3 to 10. The highest swelling ratio is obtained at pH 8, reaching 7500% for H800. Self-healing of hydrogels is evidenced by rheological measurements with alternatively applied low and high strains, and by using a macroscopic approach with re-integration of injected filaments. Furthermore, the H1900 membrane exhibits outstanding antibacterial activity against an *E. coli* suspension at 10^8 CFU mL^{-1}. Therefore, dynamic hydrogels synthesized from CMCS and Jeffamine present outstanding rheological, swelling, self-healing and antibacterial properties, and are most promising as healthcare material in wound dressing, drug delivery and tissue engineering.

1. Introduction

Hydrogels are soft materials which are capable of absorbing large amount of water without dissolution [1]. They are generally composed of a 3-dimensional hydrophilic polymer network linked together either by covalent bonds [2], or by physical interactions via chain entanglements, hydrophobic association, electrostatic interactions, van der Waals forces, etc. [3]. In the past decades, hydrogels have been most widely studied for applications in drug delivery [4], wound dressing [5], tissue engineering [6], and in agriculture [7], owing to their prominent properties such as flexibility, ductility, and biocompatibility.

Dynamic hydrogels are a new generation of hydrogels which are crosslinked by dynamic covalent bonding via S_N2-type nucleophilic substitution [8], imine chemistry [9], Diels-Alder reaction [10], etc. Generally, they are responsive to external stimuli, such as light, temperature, and pH [11–13]. A dynamic hydrogel was formed by specific benzoxaborole-carbohydrate interactions between benzoxaborole-modified hyaluronic acid and fructose-based glycopolymer. Release of doxorubicin from the hydrogel can be precisely switched on/off by near-infrared light as a trigger [11]. A thermos-sensitive hydrogel was generated by dynamic chemical oxime bonding from alkoxyamine-terminated Pluronic F127 and oxidized hyaluronic acid, as well as hydrophobic association. The hydrogel exhibits much higher modulus and higher stability than the Pluronic F127 hydrogel, and could be used as a promising postoperative anti-adhesion material in clinical practice [12]. On the other hand, soft hydrogels based on alginate-boronic acid were obtained from reversible inter- and intramolecular interactions by dynamic equilibrium of boronic acid–diol complexation and dissociation. The hydrogels present pH- and glucose-sensitivities [13], and could be promising for applications as biological glues that require stretchability, self-healing, and multi-responsive behavior. Although these dynamic hydrogels exhibit versatile stimuli-responsive properties compared to common hydrogels, the approaches involved in the hydrogel fabrication is rather complex. Thereby, among the various dynamic bonds, imine bonding attracted great interest because of mild reaction conditions [14], the efficient reversibility of imine bonds, tunable properties and stimuli-responsive performance of resulted materials [15].

Chitosan (CS) is a polysaccharide widely used to prepare hydrogels for various applications because of its biocompatibility [16], biodegradability [17], and anti-bacterial activities [18]. Recently, chitosan received much attention as a hydrophilic biopolymer for reversible crosslinking via reaction between the amino groups along the backbone and other polymers [19], including hyaluronic acid [20], alginate [21], and gelatin

* Corresponding authors.
E-mail addresses: mihail-dumitru.barboiu@umontpellier.fr (M. Barboiu), suming.li@umontpellier.fr (S. Li).

https://doi.org/10.1016/j.ijbiomac.2020.11.068.

[22]. Nevertheless, high molar mass chitosan is poorly soluble in water at neutral or basic pH due to intermolecular hydrogen bonding [23], which is not beneficial for its utilization in the biomedical field.

Carboxymethyl chitosan (CMCS) is a water-soluble derivative of chitosan which presents outstanding biological properties [24]. Crosslinking of CS or CMCS with different aldehydes has been reported, including monoaldehydes [25], dialdehydes [26], and derivatives of aldehydes [27]. The resulting hydrogels present good mechanical strength [26,28], and have been studied for applications in tissue engineering. However, these hydrogels present some disadvantages such as low swelling ratio, tedious preparation procedure, disordered micro-structure, etc.

Benzene-1,3,5-tricarbaldehyde (BTA) is a promising cross-linker for the formulation of dynamic hydrogels based on imine bonding. In fact, BTA can serve as a tri-topic center for three-dimensional cross-linking with diamino polymers, thus yielding nonlinear and continuous network structures [29]. Nevertheless, BTA is not soluble in water, which prevents its uses in aqueous medium. Jeffamine is a biocompatible polyetheramine consisting of poly(propylene oxide) (PPO) and poly (ethylene oxide) (PEO) blocks terminated with primary amino groups. It has been largely used in the synthesis of amphiphilic block copolymers [30], hydrogels [31], and dynamic frameworks [32].

Currently, with the appearance of new medical equipments and technologies, the prevention of bacteria and fungi becomes a key issue in different medical therapies. The development of antimicrobial materials attracted much interest [33], especially hydrogels possessing intrinsic antibacterial properties. For example, hydrogels based on CS or CMCS have been largely investigated as wound dressing [34].

In our previous work, a dual-imine dynamic hydrogel was prepared using a two steps procedure under mild conditions [35]. Difunctional Jeffamine ED2003 (Mn 1900) first reacts with BTA to form a water soluble dynamer (Dy), followed by crosslinking of the dynamer and CMCS in water to yield a 3-dimensional network, both based on Schiff base reaction. The resulting hydrogels present high storage modulus, pH-sensitive swelling behavior, outstanding self-healing performance and excellent cytocompatibility. In this work, dynamic hydrogels were prepared using the same procedure from three Jeffamines of different molar masses, i.e. ED600 (Mn 500), ED900 (Mn 800) and ED2003 (Mn 1900). The resulting hydrogels were characterized by Fourier-transform infrared spectroscopy (FT-IR) and rheological measurements. The pH dependent swelling and self-healing behaviors were evaluated to evidence the effect of Jeffamine molar mass on hydrogel properties. The antibacterial properties were determined to assess the potential of dynamic hydrogels in biomedical applications such as wound dressing or tissue engineering scaffold.

2. Experimental section

2.1. Materials

O,O′-Bis (2-aminopropyl) poly(propylene glycol)-*block*-poly(ethylene glycol)-*block*-poly(propylene glycol) (Jeffamine®) ED-600 (M_n 500), ED900 (M_n 800) and ED-2003 (M_n 1900) from Sigma-Aldrich, benzene-1,3,5-tricarbaldehyde (BTA) from Manchester Organics (Purity 98%) were used without further purification. *O*-carboxymethyl chitosan (CMCS) with degree of carboxymethylation of 80%, degree of deacetylation of 90%, and Mw of 200,000 Da was supplied by Goldenshell Biochemical Co., Ltd. Methanol (96%), citric acid (99.5%), disodium hydrogen phosphate dodecahydrate (99%), boric acid (99.5%), and borax (99%) were of analytical grade, and obtained from Sigma-Aldrich. All chemicals were used without further purification. *Escherichia coli* (K12 DSM 423) was purchased from DSMZ, Germany.

2.2. Synthesis of dynamers Dy500, Dy800 and Dy1900

BTA (162.14 mg, 1 mmol), Jeffamine® ED-600 (0.5 g, 1 mmol) were added in 30 mL methanol. The reaction mixture was stirred at 70 °C under reflux for 4 h. The solvent was then evaporated using rotary evaporator. 20 mL Milli-Q water was added to yield a homogeneous Dy500 solution of 50 mM, as calculated from remaining aldehyde groups. Dy800 and Dy1900 were prepared from Jeffaminie® ED-900 or ED-2003 under the same conditions.

2.3. Synthesis of hydrogels

100 mM CMCS solution was prepared by dissolving 1.06 g CMCS (5 mmol, calculated from D-glucosamine units) in 50 mL Milli-Q water at room temperature. CMCS and dynamer aqueous solutions were mixed at a glucosamine/Dy molar ratio of 4/1 to a total volume of 3 mL. The mixture was ultra-sonicated for 1 min to remove trapped bubbles. Gelation then proceeded at 37 °C for 24 h to yield a hydrogel, namely H500, H800 or H1900.

2.4. Preparation of H1900 membranes

8 mL of 100 mM CMCS and 4 mL of 50 mM Dy1900 solutions were mixed in a flask. The mixture was ultra-sonicated for 1 min to remove trapped bubbles, and poured into a round PTFE mold of 8 cm diameter. Gelation then proceeded at 37 °C for 24 h. The resulting hydrogel was air dried under natural ventilation to yield a H1900 membrane. The membrane was recovered and vacuum dried up to constant weight.

A membrane was also prepared from CMCS without crosslinking for the sake of comparison.

2.5. Characterization

^{1}H NMR spectroscopy was carried out using Bruker NMR spectrometer (400-LS) of 400 MHz. Chloroform-d_2 was used as the solvent. 5 mg of sample were dissolved in 0.5 mL of solvent for each analysis. Chemical shifts were recorded in ppm using tetramethylsilane (TMS) as internal reference.

Fourier-transform infrared (FT-IR) spectroscopy of freeze-dried hydrogels was conducted on Nicolet Nexus FT-IR spectrometer, equipped with ATR diamant Golden Gate.

The morphology of freeze-dried hydrogels was examined by using Hitachi S4800 scanning electron microscopy (SEM). As-prepared hydrogels were placed in small vials, and immersed in liquid nitrogen (−196 °C) in order to conserve the original structure. The frozen samples were then lyophilized using LABCONCO® freeze dryer for 24 h. The samples were sputter coated prior to analysis.

Physical MCR 301 Rheometer (Anton Paar) was utilized to determine the rheological properties of hydrogels, using a cone plate geometry (diameter of 4 cm, apex angle of 2°, and clearance 56 μm). The storage modulus (G′) and loss modulus (G″) were measured as a function of time, strain or frequency.

2.6. Swelling of freeze-dried gels

The swelling performance of freeze-dried gels was evaluated by immersion in buffer solutions at different pH values. Buffers from pH 1 to pH 7 were prepared from 0.1 M citric acid and 0.2 M disodium hydrogen phosphate dodecahydrate solutions, buffers at pH 8 and pH 9 from 0.2 M boric acid and 0.05 M borax solutions, and buffer at pH 10 from 0.05 M borax and 0.2 M sodium hydroxide solutions. Freeze-dried gels were immersed in a buffer solution, and taken out after 24 h. The swollen hydrogels were weighed after wiping surface water with filter paper, and weighed again after 24 h lyophilization. The swelling and mass loss ratios of hydrogels were calculated according to the following equations, respectively:

$$\text{Swelling ratio}\% = \frac{(M_s - M_d)}{M_d} \times 100 \quad (1)$$

$$\text{Mass loss ratio}\% = \frac{(M_0 - M_d)}{M_0} \times 100 \quad (2)$$

where M_0 is the initial mass of dried gel, M_s is the wet mass of the swollen hydrogel, and M_d is the dried mass of the swollen hydrogel after lyophilization.

2.7. Self-healing properties of hydrogels

Hydrogel samples were prepared in Milli-Q water. One of them was dyed red with Rhodamine B for better observation. 2 different approaches were applied to examine the self-healing behavior of hydrogels: 1) modulus changes of hydrogels were followed with alternatively applied high and low oscillatory shear strains at 37 °C; 2) hydrogels were injected in a petri dish to observe integration of filaments at 37 °C.

2.8. Antibacterial activity of membranes

2.8.1. Bacterium and preparation of the bacterial suspension

A non-pathogenic strain of *Escherichia coli* (K12 DSM 423, DSMZ, Germany) was selected as a model for bacterial contamination. A culture medium Lysogeny Broth (LB) Miller was used for growth and counting. LB agar and soft agar were obtained by adding microbiological agar (Sigma, France) into LB solution at concentrations of 15 g L^{-1} and 5 g L^{-1}, respectively. For each experiment, a new bacterial culture was prepared from frozen aliquots of *E. coli* stored at −20 °C. The aliquots were inoculated into fresh LB medium (2%, v/v), and incubated 18 h at 30 °C under constant stirring at 150 rpm until the optical density at 600 nm of the bacterial culture reached about 5 (which corresponds approximately to 10^9 CFU mL^{-1}). Bacteria were in a stationary phase in these conditions. Once prepared, the bacterial culture was centrifuged at 15,000*g* for 5 min at 4 °C to discard the culture medium, followed by washing with the same volume of 9 g L^{-1} NaCl solution in the same conditions. Finally, the washed bacteria were diluted with 9 g L^{-1} NaCl solution to yield suspensions at bacterial concentrations ranging from 10^8 to 10^5 CFU mL^{-1} for antibacterial activity tests. The bacterial concentration of the suspensions was stabilized, i.e. no growth could occur due to the absence of nutriments.

2.8.2. Antibacterial tests

H1900 membranes were exposed to two disinfection treatments before antibacterial tests, namely H1900[a] exposed to thermal treatment only (24 h at 100 °C), and H1900[b] exposed to thermal treatment followed by UVc exposure. UVc exposure was performed using a neon of the microbiological safety cabinet (Bioair, Safemate 1.2) under the following conditions: wavelength - 254 nm, power - 30 W, distance to the sample - 50 ± 5 cm, time - 30 min for each membrane side. CMCS membrane was exposed to both thermal treatment and UVc exposure.

A liquid test was firstly performed to assess the total bacterial removal, including both bacterial adsorption and inactivation. The membrane piece was immersed 3 h at ambient temperature (20 °C) in the bacterial suspension prepared in Section 2.8.1. The bacterial concentration was measured before and after contact with the membrane. An initial bacterial concentration C_0 of about 10^8 CFU mL^{-1} was used for this test. A concentration decrease was correlated to bacterial removal. The bacterial log-removal value was defined as the logarithm (base 10) ratio of the initial bacterial concentration C_0 (CFU mL^{-1}) to the bacterial concentration C (CFU mL^{-1}) measured after 3 h contact with the membrane. A log-removal value of log (C_0) was attributed to the particular case of total bacterial removal. A log-removal value of 1 corresponds to a decrease of 90% of the bacterial population, and a log-removal value of 2 corresponds to a decrease of 99% bacterial population.

The antibacterial effect of the membrane was then assessed by a soft agar test. 50 μL of the bacterial suspension (at about 10^5 CFU mL^{-1}) was deposited onto a membrane piece (between 2 and 3 cm^2) placed individually in an empty petri dish. After 3 h contact at ambient temperature (20 °C), 10 mL of nutritive LB soft agar were added, embedding the membrane in a 2 mm thick soft agar. The plates were then incubated 72 h at 30 °C to let the colonies grow. This soft agar test allows the growth of bacteria adsorbed on the membrane without damaging the membrane.

For each antibacterial test, a positive control was realized under the same conditions without membrane. All tests were duplicated.

2.8.3. Counting of viable cells

The bacteria were counted by using the conventional plaque assay method. For the liquid test, each sample was diluted in decades in a 9 g L^{-1} NaCl solution; six successive dilutions were done. Then, 400 μL of each dilution were spread onto a LB agar plate, and incubated for 72 h at 30 °C. Once the cultivable bacteria had grown on plates, the colonies were counted, keeping in mind that each colony stemmed from one initial bacterium. For the soft agar test, the colonies grown in the soft agar were directly counted. For all tests, the concentration of bacteria was calculated as the average of the counted colony number divided by the inoculated volume, taking into account the dilution factor. The quantification limit was 3 CFU mL^{-1}. Each counting was duplicated. Negative control (i.e. without bacteria) was always performed in parallel to check the sterility.

3. Results and discussion

3.1. Preparation of hydrogels

Imine dynamic hydrogels were prepared through a two steps approach as previously reported [35]. A water soluble dynamer Dy500, Dy800 or Dy1900 was first synthesized by reaction of BTA as the core structure and bifunctional Jeffamine® ED-600 (Mn = 500), ED-900 (Mn = 800) or ED-2003 (Mn = 1900) as the water-soluble linker via reversible imine chemistry (Scheme 1). The BTA to Jeffamine® molar ratio was 1:1. In other words, one aldehyde group per BTA molecule remains available for further cross-linking with the amine groups of CMCS since each BTA molecule has three aldehydes and each Jeffamine® molecule has two amines.

Fig. 1 presents the ^{1}H NMR spectra of the as-prepared dynamers obtained after 4 h reaction in methanol at 70 °C. Three signals of aldehyde groups are observed in the 10.1–10.3 ppm range (a), and attributed to different degrees of substitution in tri-aldehyde. Signals (b) between 8.0 and 8.7 ppm are assigned to the imine and aromatic protons, signals (c) around 3.5 ppm to the methylene and methine protons, and signals (d) around 1.0 ppm to the methyl protons of Jeffamine. The presence of residual H_2O is detected between 2.0 and 1.8 ppm. Signals at 5.24 ppm and 0 ppm are attributed to the chloroform-d_2 and internal standard, respectively.

In the second step, the remaining aldehyde groups of the dynamer react with the amines of CMCS, resulting in a dynamic hydrogel composed of a double imine bonding framework. This double imine crosslinking in aqueous medium is facile and eco-friendly as compared to CMCS-based hydrogel prepared by amide bond crosslinking using 1-ethyl-3(3-dimethylaminopropyl) carbodiimide as crosslinker and N-hydroxysuccinimide as activator [36]. Three series of hydrogels were prepared via a mixture of aqueous solutions of 100 mM CMCS and 50 mM Dy500, Dy800 or Dy1900 at a D-glucosamine to Dy molar ratio of 4. This ratio was used because it leads to optimal crosslinking as previously reported [35]. Gelation proceeded at 37 °C for 24 h to yield H500, H800 or H1900 hydrogels. Table 1 summarizes the molar compositions and total polymer concentrations of the three hydrogels. The total polymer concentration increases from 2.4% for H500 to 2.9% for H800, and to 4.8% for H1900.

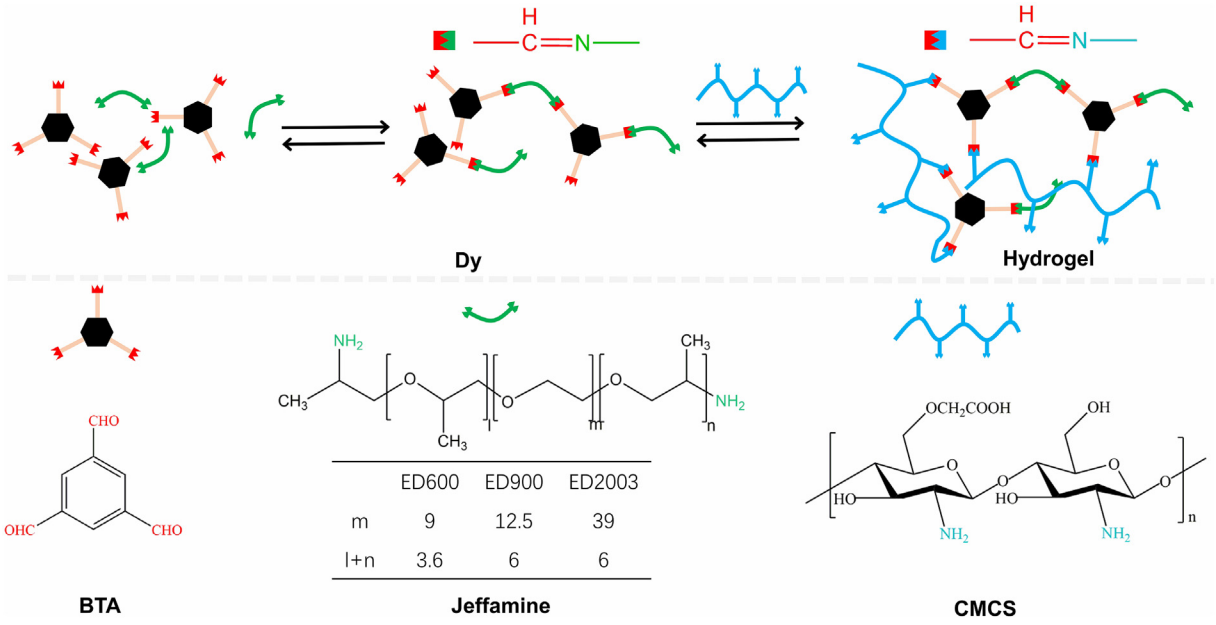

Scheme 1. Synthesis route of dynamic hydrogel by imine bond formation between CMCS and a dynamer obtained from BTA and Jeffamine.

3.2. FT-IR

Fig. 2 shows the FTIR spectra of CMCS, the dynamers and the dried gels. The large band around 3500 cm^{-1} is attributed to free OH and NH_2 groups, and the intense band at 1595 cm^{-1} to carbonyl groups of CMCS. The dynamers present large bands at 2850 and 1100 cm^{-1} belonging to C—H and C—O stretching, and two characteristic bands at 1698 and 1645 cm^{-1} corresponding to aldehyde and imine bonds, respectively. All the characteristic bands of CMCS and Dy are observed on the spectra of dried gels. Nevertheless, the enlarged view in the 1750–1550 cm^{-1} wavenumber range shows that the aldehyde band almost disappears, while the imine band merges with that of carbonyl

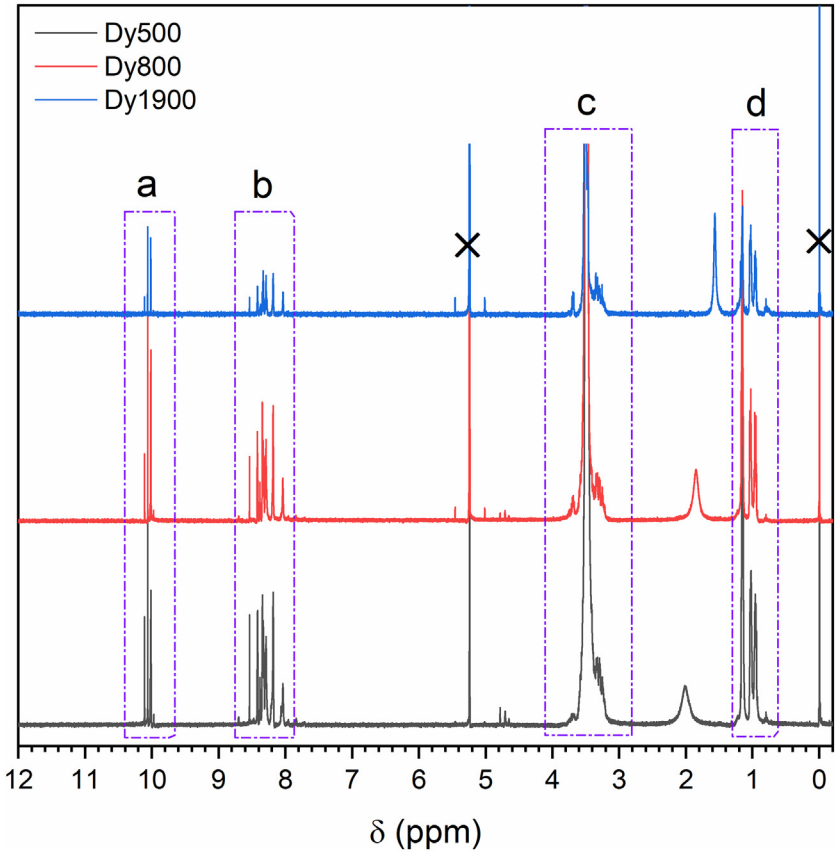

Fig. 1. ^1H NMR spectra of the dynamers Dy500, Dy800 and Dy1900 obtained by reaction of BTA and Jeffamine.

Table 1
Molar and mass compositions of dynamic hydrogels[a].

Sample	D-glucosamine/Dy molar ratio	CMCS		Dy500[b]		Dy800[b]		Dy1900[b]		Total polymer concentration
		[mmol]	[w/v %]	[mmol]	[w/v %]	[mmol]	[w/v %]	[mmol]	[w/v %]	[w/v%]
H500	4	0.2	1.4	0.05	1.0	–	–	–	–	2.4
H800	4	0.2	1.4	–	–	0.05	1.5	–	–	2.9
H1900	4	0.2	1.4	–	–	–	–	0.05	3.4	4.8

[a] Hydrogels are prepared by mixing CMCS and Dy solutions at a D-glucosamine/Dy ratio of 4/1 to a total volume of 3 mL. The concentration of CMCS solution is 100 mM. Calculations are made on the basis of the average molar mass of 212 g/mol obtained for D-glucosamine, taking into account the degree of deacetylation of 90% and the degree of carboxymethylation of 80%.
[b] The concentration of Dy solution is 50 mM obtained from the remaining aldehyde groups. In a typical reaction, 1 mmol BTA (162 mg) reacts with 1 mmol Jeffamine ED600 (500 mg) or Jeffamine ED900 (800 mg) or Jeffamine ED2003 (1900 mg) to form a dynamer. As BTA has 3 aldehydes and Jeffamine 2 amines, there remains theoretically 1 mmol of aldehydes in the dried dynamer. Addition of 20 mL water yields a dynamer solution of 50 mM.

groups at 1595 cm^{-1}. These results indicate that hydrogels are formed owing to imine formation through aldehyde and amine groups.

3.3. Rheology

The gelation of dynamic hydrogels was investigated by rheological measurements. CMCS and Dy aqueous solutions were mixed in situ on the plate of the rheometer, and changes of the storage modulus (G′) and loss modulus (G″) were followed as a function of time at 37 °C (Fig. 3a). For all samples, G' is initially lower than G″, which illustrates a liquid-like behavior of the starting mixture. After an induction time, both G′ and G″ begin to increase, G′ increasing faster than G″. A cross-over point of G′ and G″ is detected, indicating sol-gel transition. The gelation time of H500, H800 and H1900 is 210 s, 300 s, and 360 s, respectively, with corresponding modulus of 0.15 Pa, 0.20 Pa, and 1.46 Pa at the gelation point. Thus, low molar mass of Jeffamine is beneficial for rapid gelation, but leads to lower modulus of as-prepared hydrogels.

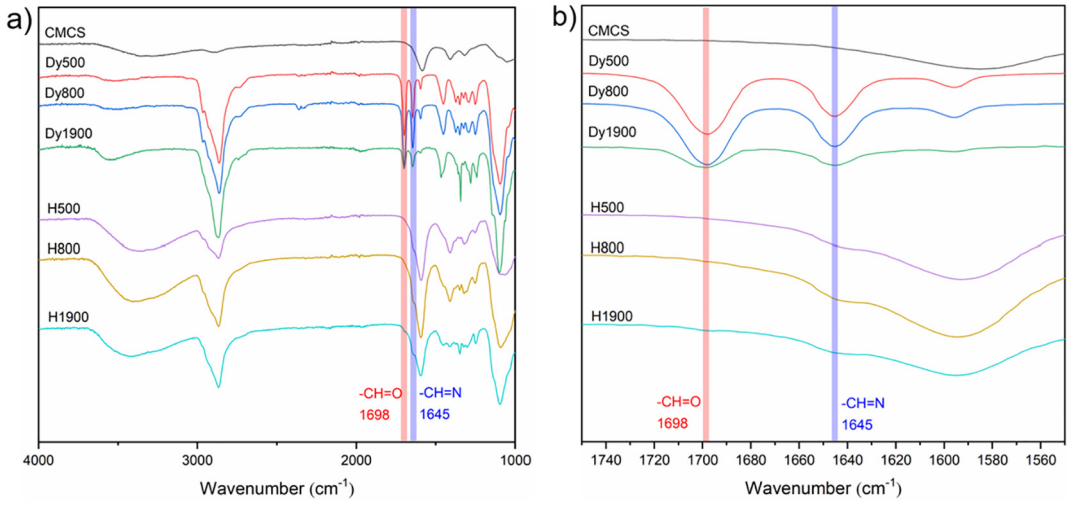

Fig. 2. a) FT-IR spectra, and b) enlarged view of the 1550–1750 cm^{-1} wavenumber range of CMCS, Dy500, Dy800, Dy1900, H500, H800 and H1900.

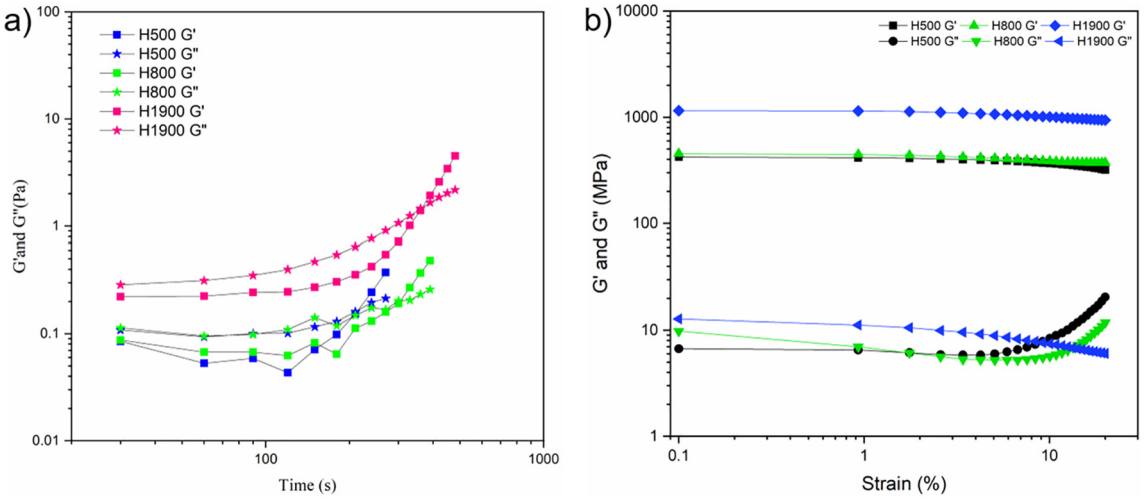

Fig. 3. a) Storage modulus (G′) and loss modulus (G″) changes as a function of time after mixing CMCS with Dy solutions at 37 °C, at strain of 1% and frequency of 1 Hz; b) storage modulus (G′) and loss modulus (G″) changes of H500, H800 and H1900 as a function of strain at 25 °C and 1 Hz.

Fig. 3b presents the modulus changes of as prepared hydrogels as a function of applied strain at 25 °C and at 1 Hz. G′ is nearly stable over the whole strain range up to 20% although a slight G′ decrease is detected at high strains. On the other hand, the loss modulus G″ is much lower than the storage modulus G′ in all cases, indicating viscoelastic behavior rather than liquid behavior of hydrogels. In fact, a linear viscoelastic range is generally observed for chemically or physically crosslinked hydrogels [36–38].

When the Jeffamine molar mass increases from 500 to 800, the storage modulus slightly increases from 422 Pa for H500 to 453 Pa for H800 at 1% strain. In contrast, much higher G′ of 1190 Pa is obtained for H1900. This finding indicates that the molar mass of Jeffamine strongly influences the mechanical properties of hydrogels. Higher molar mass of Jeffamine leads to higher modulus of hydrogels. In fact, although there are more amine groups than aldehyde ones in the mixture, the amines are less available for imine chemistry than aldehydes due to their lower chain mobility and steric effect as they are present along the CMCS backbone with a Mw of 200,000. Thus, a D-glucosamine to Dy molar ratio of 4 was used for optimal crosslinking. Similar findings were obtained for modulus changes of as prepared hydrogels as a function of applied frequency from 0.1 to 50 Hz at 25 °C and at 1% strain (Fig. S1). It is noteworthy that these dynamic hydrogels present better

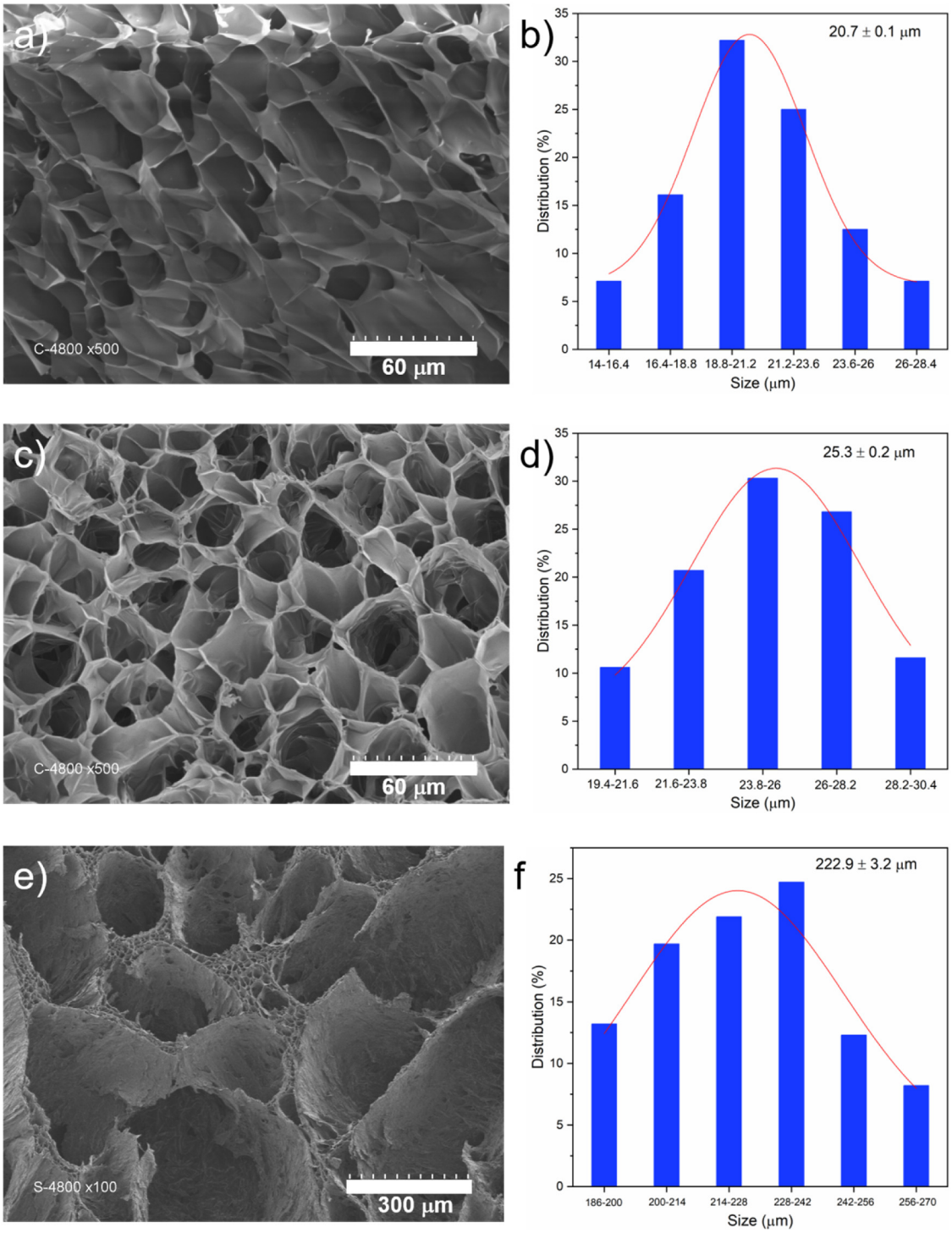

Fig. 4. SEM images and pore size distributions of freeze-dried gels: (a, b) H500; (c, d) H800; (e, f) H1900.

mechanical performance than CMCS-based hydrogels by amide bond crosslinking [36].

3.4. Morphology and swelling performance

The inner structure of freeze-dried hydrogels was examined using SEM. As shown in Fig. 4, H500, H800 and H1900 exhibit a sponge-like porous structure with regularly distributed and interconnected pores, which is beneficial for utilization in drug delivery or tissue engineering as compared to irregular microstructure of other chitosan hydrogels [39]. Noticeably, the average pore size varies from 20.7 ± 0.1 μm for H500, to 25.3 ± 0.2 μm for H800, and to 222.9 ± 3.2 μm for H1900. This finding suggests that the molar mass of Jeffamine significantly affect the three-dimensional architecture of hydrogels, especially on the pore size. Higher Jeffamine molar mass leads to larger pore size because Jeffamine molecules serve as linkers in the hydrogel network.

The swelling behavior of hydrogels is of major importance for medical applications in wound dressing, drug delivery or tissue engineering. It is thus of interest to compare the swelling of hydrogels prepared from different Jeffamines. As shown in Fig. 5a, the swelling ratio is strongly pH dependent as previously reported [35]. In acidic media at pH 3 and 4, the swelling ratio is rather low (between 200 and 300%). In slightly acidic and neutral media (pH 5, 6, 7 and 7.4), the swelling ratio progressively increases to reach *c.a* 2000%. Maximal swelling is observed in slightly basic media at pH 8, with a swelling ratio of 5280%, 7560% and 5590% for H500, H800, and H1900, respectively. With further increase to pH 9 and 10, however, the swelling ratio decreases, reaching 2710%, 3500% and 2250% for H500, H800, and H1900 at pH 10, respectively. The pH dependence of the swelling of hydrogels is attributed to electrostatic interactions resulted from the presence of amino and carboxyl groups along CMCS chains [35]. In fact, strong electrostatic attraction occurs between negatively charged -COO^- and positively charged -NH_3^+ groups in strong acidic media (pH 3 and 4), leading to shrinkage of hydrogels and low swelling ratio. Electrostatic attraction becomes weaker at slightly acidic or neutral pH, and thus the swelling ratio increases. In contrast, strong electrostatic repulsion occurs between negatively charged -COO^- groups in slightly alkaline medium at pH 8, resulting in strong swelling. With further increase of alkalinity, however, the electrostatic repulsion between the -COO^- groups is counterbalanced by the OH^- ions in solution. Hence, the swelling of hydrogels at pH 9 and 10 diminishes compared to that at pH 8. No major difference was observed between the three hydrogels in acidic and neutral media, although H800 seems to present higher swelling ratio than H500 and H1900 in alkaline media. Additionally, compared to other chitosan-based hydrogel [36], the excellent swelling ability of these dynamic hydrogels should be beneficial for absorption of interstitial fluid or wound exudate, and thus enlarging their biomedical utilization, especially as wound dressing [40].

Mass loss often occurs during swelling of hydrogels due to the solubilization of non-crosslinked species. Thus, the mass loss ratio is an indicator of the crosslinking degree and the stability of hydrogels. Fig. 5b presents the mass loss ratio of hydrogels at different pH values. Noticeably, the mass loss of hydrogels is strongly pH dependent. High mass loss above 50% is obtained in acidic buffers at pH 3 and 4. From pH 5 to pH 7.4, the mass loss ratio progressively decreases. And in alkaline media, a slight increase of mass loss is observed. These findings suggest that the imine bonds in the hydrogel network are partly hydrolyzed in acidic media, especially at pH 3 and 4. In contrast, they are stable in neutral and alkaline media. The slight increase of mass loss in alkaline media could be assigned to the high swelling which facilitated the washing away of uncross-linked species. Among the three hydrogels, H1900 exhibits the highest mass loss in the whole pH range, in agreement with lower crosslinking degree due to the higher molar mass of Jeffamine ED2003. In fact, better crosslinking could be achieved between CMCS and Dy500 or Dy800 based on Jeffamine ED600 and ED900 of lower molar masses. This hypothesis is supported by the fact that H500 exhibits the lowest mass loss ratio in the range from pH 5 to 9, with a minimum mass loss ratio of 8% at pH 7.

3.5. Self-healing

The prepared dynamic hydrogel exhibits self-healing behavior as evidenced by rheological measurements at fixed frequency of 1 Hz and at 37 °C. Fig. 6a shows modulus changes of H1900 as a function of applied strain. With increasing strain, the storage modulus of H1900 remains stable till a strain of 30%. Beyond, G′ rapidly decreases. On the other hand, the loss modulus begins to increase beyond 10% strain. A crossover point is detected at a stain of 62%, indicating the collapse of the hydrogel structure.

Continuous step strain measurements were then performed to verify the rheological self-recovery of H1900 with alternatively applied low and high strains. As shown in Fig. 6b, at a strain of 1%, H1900 behaves as a hydrogel since G′ is highly superior to G″ in spite of some G′ decrease. Then the oscillatory shear strain was increased to 62% and maintained for 100 s. Both G′ and G″ almost overlap. With the shear strain back to 1%, H1900 behaves again like a hydrogel with both G′ and G″ remaining stable. Similar measurements were made by alternatively applying higher strains (100, 200 and 300%) and low strain (1%). At high strains, G′ is lower than G″ due to collapse of the hydrogel structure. And at 1% strain, G′ almost recovers its initial value. Similar

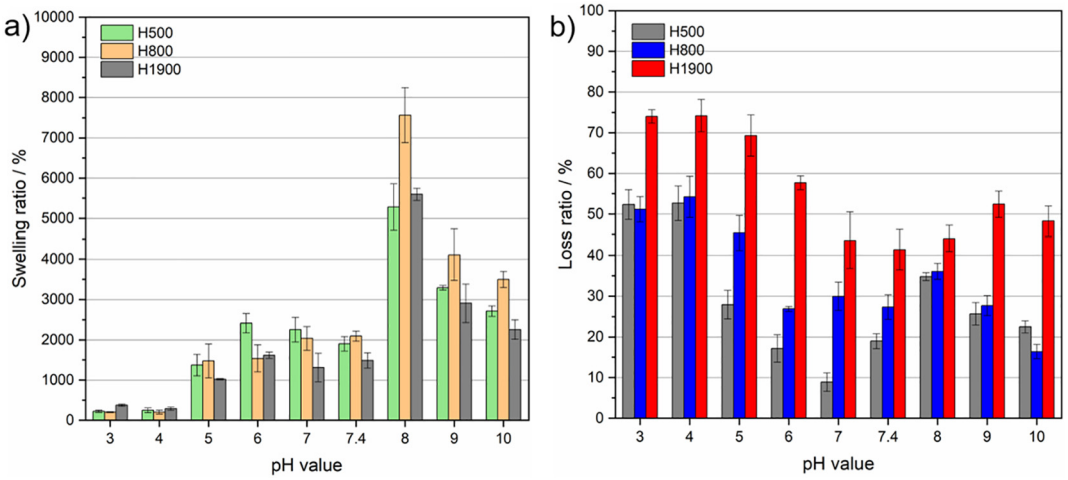

Fig. 5. a) Equilibrium swelling ratios, and b) mass loss ratios of H500, H800 and H1900 after 24 h immersion in buffers at various pH values.

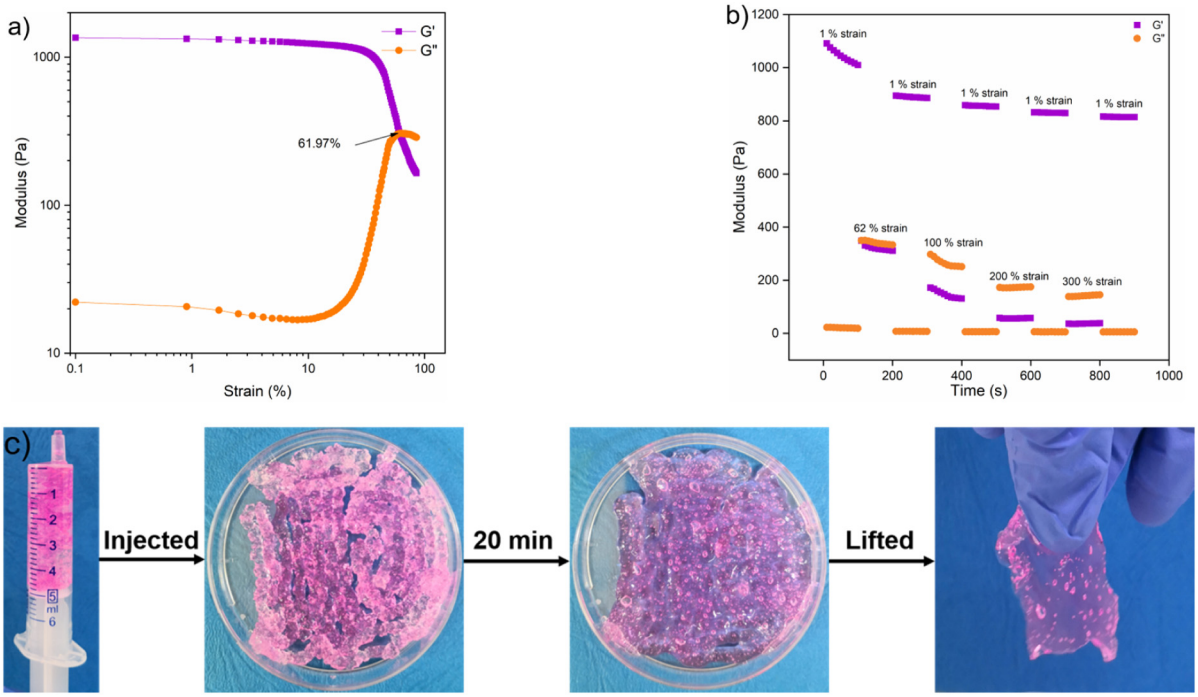

Fig. 6. a) Modulus changes as a function of strain of H1900 prepared in Milli-Q water; b) modulus changes of H1900 prepared in Milli-Q water with alternatively applied high and low oscillatory shear strains at 37 °C; c) macroscopic observation of self-healing of H1900 at 37 °C.

behaviors are observed for H500 and H800 with alternatively applied low and high strains. Therefore, rheological measurements clearly evidence the self-recovery properties of dynamic hydrogels owing to the reconstruction of reversible crosslinking in the hydrogel network, which makes them promising for applications in cell therapy, tumor therapy and even in bone repairing [41].

A macroscopic approach was used to further illustrate the self-healing of imine dynamic hydrogels, by using a hydrogel sample dyed red with Rhodamine B for better visualization (Fig. 6c). The sample was injected onto a plastic petri dish through a syringe and placed as filaments side by side. The filaments became almost integrated only after 20 min, and was easily peeled from the petri dish and lifted by hand.

3.6. In vitro antibacterial assay

Chitosan based materials present intrinsic antimicrobial properties due to the presence of amino groups [42]. Considering the overall properties of the three hydrogels, H1900 was selected for in vitro antibacterial activity studies by using *E. coli* (Gram-negative bacterium). H1900 membranes were first subjected to two sterilization treatments, i.e. H1900^{a} exposed to thermal treatment only and H1900^{b} exposed to thermal treatment followed by UVc exposure so as to examine the effect of UV on the membrane properties [43]. The membranes were characterized by FT-IR analysis in comparison with pristine H1900 (Fig. S2). The results show that the thermal treatment and the UVc exposure have no major impact on the chemical structure of membrane since the main functional groups remained the same without apparent peak shift, implying the good stability of H1900 membranes. UVc treatment for sterilization of CMCS-based biomaterials is therefore acceptable after thermal treatment.

Fig. 7 shows the bacterial concentrations obtained in liquid tests for H1900^{a} and H1900^{b} in comparison with CMCS membrane and positive control. After 3 h contact at ambient temperature (20 °C) with a bacterial suspension at 10^{8} CFU mL^{-1}, the positive control and CMCS membrane present small log-removal values, i.e. 0.2 and 0.1, respectively (Table 2, entries 2 and 5). On the contrary, the H1900 membranes exhibit significant log-removal values, i.e. 1.5 for H1900^{a} and 5.6 for H1900^{b} (Table 2, entries 3 and 4). In other words, 97.11% and 99.9999% of bacteria were removed by H1900^{a} and H1900^{b}, respectively, suggesting outstanding antibacterial properties of H1900. The antibacterial activity of the hydrogel could be assigned to the positively charged amino groups along the CMCS chains which could bind to the negatively charged phospholipid groups present on the bacterial membranes, thus inducing membrane permeabilization, release of the intracellular fluids and finally cell death [42,44]. Additionally, the Schiff-base containing a benzene ring could also play a significant role in the

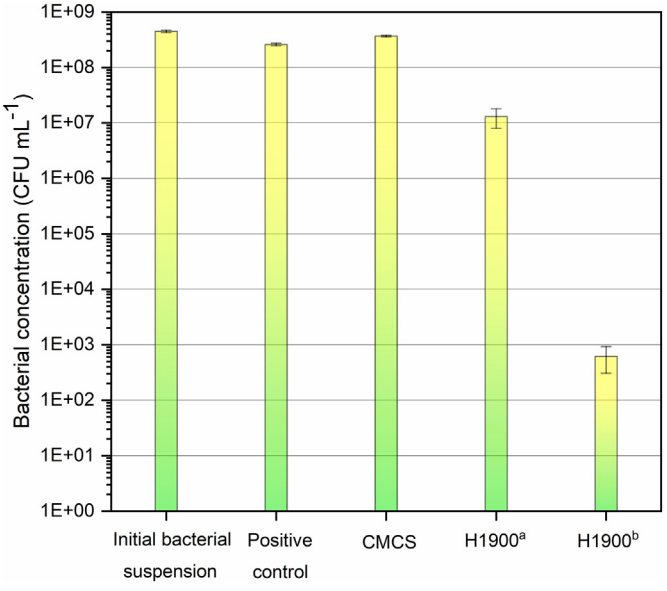

Fig. 7. Bacterial concentrations (CFU mL^{-1}) obtained for positive control, CMCS, H1900^{a}, and H1900^{b} in liquid tests (H1900^{a} with only thermal treatment for sterilization, H1900^{b} with both thermal treatment and UVc exposure for sterilization).

Table 2
Antibacterial activity of H1900 membranes (entry 1–5: liquid test; entries 6–9: soft agar tests).

Entry	Sample	$C_{bacteria}$ [CFU mL^{-1}]	Log-removal value [−]
1	Initial bacterial suspension	$4.5 \pm 0.2 * 10^8$	–
2	Positive control	$2.6 \pm 0.1 * 10^8$	0.2
3	H1900[a]	$1.3 \pm 0.5 * 10^7$	1.5
4	H1900[b]	$6.2 \pm 3.1 * 10^2$	5.6
5	CMCS	$3.7 \pm 0.1 * 10^8$	0.1
6	Positive control	$2.1 \pm 0.7 * 10^5$	–
7	H1900[a]	$5.0 \pm 3.0 * 10^1$	4.0
8	H1900[b]	0	5.3
9	CMCS	nd	nd

nd: not determined (too many bacteria).
H1900[a]: only thermal treatment for sterilization.
H1900[b]: both thermal treatment and UVc exposure for sterilization.

antimicrobial activity since Schiff-base bonds in the hydrogel network have been demonstrated as a promising candidate for designing more efficient antimicrobial agents [45]. Hence, the Schiff bases and protonated amino groups are supposed to impart outstanding antibacterial activity to H1900 membrane.

The biocidal activity of H1900[b] appears better than H1900[a] in liquid tests (Fig. 7 and Table 2), even though UVc exposure seemed not to induce major changes in the chemical structure of H1900 membrane (Fig. S2). Nevertheless, it has been reported that UV radiation could decrease the degree of deacetylation of chitosan [46]. On the other hand, the antibacterial activity of CMCS based materials is dependent on the amount of NH_3^+ groups [42,44], and thus on the degree of deacetylation. Therefore, it can be assumed that the antibacterial activity of H1900[b] is improved by UVc exposure as compared to H1900[a] exposed to thermal treatment only.

Soft agar tests were carried out in order to make sure that bacteria were effectively deactivated rather than adsorbed on the membrane. Indeed, if present, adsorbed bacteria would form colonies onto the membrane that could be observed after 72 h incubation at 30 °C. As shown in Table 2 (entries 6 and 8) and Fig. 8, the bacterial concentration is zero CFU mL^{-1} for H1900[b] with corresponding log-removal value of 5.3. In other words, no colonies grew onto the H1900[b] membrane, in contrast to the positive control (Fig. 8). Besides, the log-removal value is very close to that obtained in the liquid test (Table 2, entry 4). It is thus concluded that the bacterial removal observed in the liquid test mainly results from the antibacterial action of H1900[b] membrane, not from adsorption.

In the same way, the H1900[a] membrane exhibits a significant log-removal value of 4.0 (Table 2, entry 7), thus confirming the intrinsic and strong bactericidal activity of H1900 membranes. On the contrary, the CMCS membrane exhibits too many bacteria on a small surface for bacterial counting (Table 2), suggesting that CMCS does not have any biocidal action in these conditions probably due to membrane dissolution. It is also worth noticing that the log-removal value obtained for H1900[a] in soft agar test (Table 2, entry 7) is much higher than that obtained in the liquid test (Table 2, entry 3). This result is consistent with the assumption that the physical structure of H1900[a] allows a limited contact with bacteria when it is in suspension in a liquid, while in soft agar test, bacteria are directly deposited onto the membrane surface.

4. Conclusions

In this work, three pH-sensitive dynamic hydrogels, namely, H500, H800 and H1900, are prepared by dual-imine bond crosslinking: a dynamer is first synthesized from BTA with Jeffamine ED600, ED900 or ED2003 of different molar masses, and then the remaining aldehydes of dynamer react with the amines of CMCS to yield a hydrogel network. The gelation process is environmental-friendly without involving any organic solvent. The hydrogels present a highly porous structure with regularly distributed pores, the pore size increasing with the molar mass of Jeffamine which serves as the linker in the hydrogel network. H1900 also exhibits higher storage and loss moduli as compared to H500 and H800. The swelling and mass loss of hydrogels are highly pH sensitive due to electrostatic attraction or repulsion in buffers at various pH values. H1900 exhibits the highest mass loss probably due to the lower crosslinking degree because of the higher molar mass of Jeffamine linker. The hydrogels are more stable in neutral and alkaline media than in acidic media which facilitate the cleavage of imine bonds. The hydrogels also present excellent self-healing and antibacterial properties, and are thus most promising for biomedical applications in wound dressing, drug delivery and tissue engineering.

CRediT authorship contribution statement

Rui Yu: author who did almost all experiments, and wrote the manuscript.

Louis Cornette de Saint-Cyr: author who did the antibacterial experiments, and wrote the antibacterial part.

Laurence Soussan: author who designed the antibacterial experiments, and revised this part.

Mihail Barboiu: author who co-initiated the work.

Suming Li: author who initiated the work, supervised the whole work, and revised the manuscript.

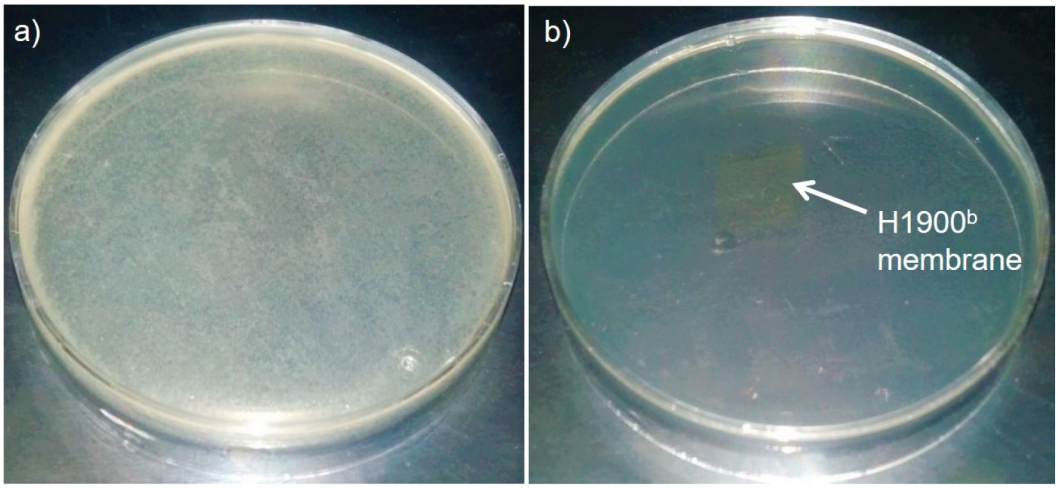

Fig. 8. Soft agar tests: a) positive control, and b) H1900[b] membrane (exposed to both thermal treatment and UV exposure for sterilization).

Acknowledgement

This work is supported by the scholarship from China Scholarship Council (CSC), and the Institut Européen des Membranes (Exploratory project "Biostent - Health" of the Internal IEM Call 2017).

Appendix A. Supplementary data

Supplementary data to this article can be found online at https://doi.org/10.1016/j.ijbiomac.2020.11.068.

References

[1] S. Van Vlierberghe, P. Dubruel, E. Schacht, Biopolymer-based hydrogels as scaffolds for tissue engineering applications: a review, Biomacromolecules 12 (5) (2011) 1387–1408.
[2] N.A. Peppas, J.Z. Hilt, A. Khademhosseini, R. Langer, Hydrogels in biology and medicine: from molecular principles to bionanotechnology, Adv. Mater. 18 (11) (2006) 1345–1360.
[3] N. Bhattarai, J. Gunn, M. Zhang, Chitosan-based hydrogels for controlled, localized drug delivery, Adv. Drug Del. Rev. 62 (1) (2010) 83–99.
[4] M. Norouzi, B. Nazari, D.W. Miller, Injectable hydrogel-based drug delivery systems for local cancer therapy, Drug Discov. Today 21 (11) (2016) 1835–1849.
[5] H. Hamedi, S. Moradi, S.M. Hudson, A.E. Tonelli, Chitosan based hydrogels and their applications for drug delivery in wound dressings: a review, Carbohydr. Polym. 199 (2018) 445–460.
[6] M. Liu, X. Zeng, C. Ma, H. Yi, Z. Ali, X. Mou, S. Li, Y. Deng, N. He, Injectable hydrogels for cartilage and bone tissue engineering, Bone Research 5 (1) (2017) 1–20.
[7] B. Qu, Y. Luo, Chitosan-based hydrogel beads: preparations, modifications and applications in food and agriculture sectors-a review, Int. J. Biol. Macromol. 152 (2020) 437–448.
[8] S. Kulchat, J.M. Lehn, Dynamic covalent chemistry of nucleophilic substitution component exchange of quaternary ammonium salts, Chemistry-An Asian Journal 10 (11) (2015) 2484–2496.
[9] L. Marin, B. Simionescu, M. Barboiu, Imino-chitosan biodynamers, Chem. Commun. 48 (70) (2012) 8778–8780.
[10] N. Roy, J.M. Lehn, Dynamic covalent chemistry: a facile room-temperature, reversible, Diels-Alder reaction between anthracene derivatives and N-phenyltriazolinedione, Chemistry-An Asian Journal 6 (9) (2011) 2419–2425.
[11] P. Sun, T. Huang, X. Wang, G. Wang, Z. Liu, G. Chen, Q. Fan, Dynamic-covalent hydrogel with NIR-triggered drug delivery for localized chemo-photothermal combination therapy, Biomacromolecules 21 (2) (2019) 556–565.
[12] Z.Y. Li, L.X. Liu, Y.M. Chen, Dual dynamically crosslinked thermosensitive hydrogel with self-fixing as a postoperative anti-adhesion barrier, Acta Biomater. 110 (2020) 119–128.
[13] S.H. Hong, S. Kim, J.P. Park, M. Shin, K. Kim, J.H. Ryu, H. Lee, Dynamic bonds between boronic acid and alginate: hydrogels with stretchable, self-healing, stimuli-responsive, remoldable, and adhesive properties, Biomacromolecules 19 (6) (2018) 2053–2061.
[14] M.G. Dekamin, M. Azimoshan, L. Ramezani, Chitosan: a highly efficient renewable and recoverable bio-polymer catalyst for the expeditious synthesis of α-amino nitriles and imines under mild conditions, Green Chem. 15 (3) (2013) 811–820.
[15] Y. Zhang, M. Barboiu, Constitutional dynamic materials toward natural selection of function, Chem. Rev. 116 (3) (2015) 809–834.
[16] F.-L. Mi, Y.-C. Tan, H.-F. Liang, H.-W. Sung, In vivo biocompatibility and degradability of a novel injectable-chitosan-based implant, Biomaterials 23 (1) (2002) 181–191.
[17] R. Dong, X. Zhao, B. Guo, P.X. Ma, Self-healing conductive injectable hydrogels with antibacterial activity as cell delivery carrier for cardiac cell therapy, ACS Appl. Mater. Interfaces 8 (27) (2016) 17138–17150.
[18] N. Sudarshan, D. Hoover, D. Knorr, Antibacterial action of chitosan, Food Biotechnol. 6 (3) (1992) 257–272.
[19] N. Bhattarai, J. Gunn, M. Zhang, Chitosan-based hydrogels for controlled, localized drug delivery, Adv. Drug Deliv. Rev. 62 (1) (2010) 83–99.
[20] H. Tan, C.R. Chu, K.A. Payne, K.G. Marra, Injectable in situ forming biodegradable chitosan-hyaluronic acid based hydrogels for cartilage tissue engineering, Biomaterials 30 (13) (2009) 2499–2506.
[21] Y.-H. Lin, H.-F. Liang, C.-K. Chung, M.-C. Chen, H.-W. Sung, Physically crosslinked alginate/N, O-carboxymethyl chitosan hydrogels with calcium for oral delivery of protein drugs, Biomaterials 26 (14) (2005) 2105–2113.
[22] Y. Li, J. Rodrigues, H. Tomas, Injectable and biodegradable hydrogels: gelation, biodegradation and biomedical applications, Chem. Soc. Rev. 41 (6) (2012) 2193–2221.
[23] L. Pighinelli, M. Kucharska, Chitosan-hydroxyapatite composites, Carbohydr. Polym. 93 (1) (2013) 256–262.
[24] R.A. Muzzarelli, Chitins and chitosans for the repair of wounded skin, nerve, cartilage and bone, Carbohydr. Polym. 76 (2) (2009) 167–182.
[25] M.M. Iftime, G.L. Ailiesei, E. Ungureanu, L. Marin, Designing chitosan based ecofriendly multifunctional soil conditioner systems with urea controlled release and water retention, Carbohydr. Polym. 223 (2019), 115040, .
[26] W. Huang, Y. Wang, Z. Huang, X. Wang, L. Chen, Y. Zhang, L. Zhang, On-demand dissolvable self-healing hydrogel based on carboxymethyl chitosan and cellulose nanocrystal for deep partial thickness burn wound healing, ACS Appl. Mater. Interfaces 10 (48) (2018) 41076–41088.
[27] A.R. Karimi, M. Tarighatjoo, G. Nikravesh, 1, 3, 5-Triazine-2, 4, 6-tribenzaldehyde derivative as a new crosslinking agent for synthesis of pH-thermo dual responsive chitosan hydrogels and their nanocomposites: swelling properties and drug release behavior, Int. J. Biol. Macromol. 105 (2017) 1088–1095.
[28] W.J. Huang, Y.X. Wang, L.M. McMullen, M.T. McDermott, H.B. Deng, Y.M. Du, L.Y. Chen, L.N. Zhang, Stretchable, tough, self-recoverable, and cytocompatible chitosan/cellulose nanocrystals/polyacrylamide hybrid hydrogels, Carbohydr. Polym. 222 (2019) 12.
[29] Y. Zhang, Y. Qi, S. Ulrich, M. Barboiu, O. Ramström, Dynamic covalent polymers for biomedical applications, Materials Chemistry Frontiers 4 (2) (2020) 489–506.
[30] A. Lu, E. Petit, S. Li, Y. Wang, F. Su, S. Monge, Novel thermo-responsive micelles prepared from amphiphilic hydroxypropyl methyl cellulose-block-JEFFAMINE copolymers, Int. J. Biol. Macromol. 135 (2019) 38–45.
[31] G. Chen, L.V.D. Does, A. Bantjes, Investigations on vinylene carbonate. VI. Immobilization of alkaline phosphatase onto poly (vinylene carbonate)-jeffamine® hydrogel beads, J. Appl. Polym. Sci. 48 (7) (1993) 1189–1198.
[32] Y. Zhang, Y. Qi, S. Ulrich, M. Barboiu, O. Ramström, Dynamic covalent polymers for biomedical applications, Materials Chemistry Frontiers 4 (2) (2020) 489–506.
[33] S. Li, S. Dong, W. Xu, S. Tu, L. Yan, C. Zhao, J. Ding, X. Chen, Antibacterial hydrogels, Advanced Science 5 (5) (2018) 1700527.
[34] M. Kong, X.G. Chen, K. Xing, H.J. Park, Antimicrobial properties of chitosan and mode of action: a state of the art review, Int. J. Food Microbiol. 144 (1) (2010) 51–63.
[35] R. Yu, Y. Zhang, M. Barboiu, M. Maumus, D. Noël, C. Jorgensen, S. Li, Biobased pH-responsive and self-healing hydrogels prepared from O-carboxymethyl chitosan and a 3-dimensional dynamer as cartilage engineering scaffold, Carbohydr. Polym. (2020) 116471.
[36] F. Su, J. Wang, S. Zhu, S. Liu, X. Yu, S. Li, Synthesis and characterization of novel carboxymethyl chitosan grafted polylactide hydrogels for controlled drug delivery, Polym. Adv. Technol. 26 (8) (2015) 924–931.
[37] F. Li, S. Li, A. El Ghzaoui, H. Nouailhas, R. Zhuo, Synthesis and gelation properties of PEG-PLA-PEG triblock copolymers obtained by coupling monohydroxylated PEG-PLA with adipoyl chloride, Langmuir 23 (5) (2007) 2778–2783.
[38] F. Li, S. Li, M. Vert, Synthesis and rheological properties of polylactide/poly (ethylene glycol) multiblock copolymers, Macromol. Biosci. 5 (11) (2005) 1125–1131.
[39] M. Hamdi, R. Nasri, S. Li, M. Nasri, Bioinspired pH-sensitive riboflavin controlled-release alkaline hydrogels based on blue crab chitosan: study of the effect of polymer characteristics, Int. J. Biol. Macromol. 152 (2020) 1252–1264.
[40] R. Jayakumar, M. Prabaharan, P.S. Kumar, S. Nair, H. Tamura, Biomaterials based on chitin and chitosan in wound dressing applications, Biotechnol. Adv. 29 (3) (2011) 322–337.
[41] Y. Xu, Y. Li, Q. Chen, L. Fu, L. Tao, Y. Wei, Injectable and self-healing chitosan hydrogel based on imine bonds: design and therapeutic applications, Int. J. Mol. Sci. 19 (8) (2018) 2198.
[42] J. Qu, X. Zhao, Y. Liang, T. Zhang, P.X. Ma, B. Guo, Antibacterial adhesive injectable hydrogels with rapid self-healing, extensibility and compressibility as wound dressing for joints skin wound healing, Biomaterials 183 (2018) 185–199.
[43] L. Huang, J. Peng, M. Zhai, J. Li, G. Wei, Radiation-induced changes in carboxymethylated chitosan, Radiation Physics Chemistry & Biodiversity 76 (11–12) (2007) 1679–1683.
[44] K.A. Brogden, Antimicrobial peptides: pore formers or metabolic inhibitors in bacteria? Nat. Rev. Microbiol. 3 (3) (2005) 238–250.
[45] M. Mohy Eldin, E. Soliman, A. Hashem, T. Tamer, Antimicrobial activity of novel aminated chitosan derivatives for biomedical applications, Adv. Polym. Technol. 31 (4) (2012) 414–428.
[46] A. Sionkowska, H. Kaczmarek, M. Wisniewski, J. Skopinska, S. Lazare, V. Tokarev, The influence of UV irradiation on the surface of chitosan films, Surf. Sci. 600 (18) (2006) 3775–3779.